Bioorganic Chemistry 89 (2019) 102990

Contents lists available at ScienceDirect

Bioorganic Chemistry

journal homepage: www.elsevier.com/locate/bioorg

Design and synthesis of dye-conjugated hepsin inhibitors

Kyul Kim[a,1], Hongmok Kwon[a,1], Doyoung Choi[a], Taehyeong Lim[a], Il Minn[b], Sang-Hyun Son[a,*], Youngjoo Byun[a,*]

[a] College of Pharmacy, Korea University, 2511 Sejong-ro, Sejong 30019, Republic of Korea
[b] Russell H. Morgan Department of Radiology and Radiological Science, Johns Hopkins Medical Institutions, Baltimore, MD 21287, United States

ARTICLE INFO

Keywords:
Hepsin
Optical dye
BODIPY
SulfoCy7

ABSTRACT

Hepsin is a type II serine protease that is highly expressed in neoplastic prostate. It is an attractive biomarker for imaging metastatic prostate cancer because of its overexpression in advanced prostate cancer and the location of its active site on the cell surface. We designed and synthesized novel hepsin-targeted imaging probes by conjugating the hepsin-binding ligand with near-infrared (NIR) optical dyes. The Leu-Arg dipeptides, attached to BODIPY or SulfoCy7, exhibited strong hepsin-inhibitory activities with K_i values of 21 and 22 nM, respectively. Compound **2** showed selective uptake and retention in hepsin-overexpressing cells. This is the first report of hepsin-targeted optical probes with strong binding affinities and high selectivity over matriptase. Compound **2** has the potential to be used for developing hepsin-based imaging probes and be as a prototype molecule in the design of new hepsin inhibitors.

1. Introduction

Prostate cancer is the most common cancer and the second leading cause of cancer death among men in USA and Europe [1]. Although surgery and radiation therapy improved the 5-year survival rate of men with prostate cancer [2], it is influenced significantly by the stage of disease progression. In particular, metastasis of locally-restricted prostate cancer into bone, lymph node, and lung dramatically increases the mortality rate [3]. Most men are diagnosed at advanced stages of prostate cancer, perhaps due to the lack of early and effective detection methods of metastatic prostate cancer [4,5]. Effective and early detection method of metastatic prostate cancer plays a crucial role in the development of therapeutic agents for advanced prostate cancer [6,7]. Consequently, there is an urgent need to develop molecular imaging modalities specifically more accurate for the detection of small lesions or metastatic sites in the early stages of prostate cancer [8].

Near-infrared (NIR) fluorescence imaging has emerged as a powerful tool in molecular imaging and cancer biology due to high sensitivity, real- time scanning capability, high compatibility with image-guided surgery, and cost efficiency [9]. Key to NIR fluorescence imaging is the use of NIR fluorophores with optimal emission excitation and emission wavelength (650–900 nm), at which biological tissues possess low absorption, minimal auto-fluorescence, and reduced scattering [10,11]. NIR imaging has a high signal-to-noise ratio in many cases [10,11]. Furthermore, NIR fluorescence light is invisible to the human eye and can be applied as a sensitive and real-time imaging tool [11]. Conventional approaches that use NIR fluorophore-labeled agents for cancer imaging require them to be chemically conjugated with cancer-specific targeting molecules such as metabolic substrates, cell-surface peptides, growth factors, antibodies, and cancer-specific biomarkers [12–15].

Prostate-specific antigen (PSA) is the most widely used biomarker for early screening of prostate cancer [16,17]. However, PSA has several limitations since it is expressed by both normal prostate cells and cancerous prostate cells [18–20]. The low specificity of PSA for prostate cancer results in over-diagnosis of indolent cancers and unnecessary biopsies. In addition, prostate cancers with smaller prostate glands and low circulating PSA are missed.

Hepsin is a type II transmembrane serine protease that is predominantly expressed in neoplastic prostate compared with benign prostate [21–25]. The expression level of hepsin mRNA are significantly elevated in > 90% of prostate cancer specimens and display > 10-fold increased levels in metastatic prostate cancer in comparison with normal prostate or benign prostatic hyperplasia (BPH) [23,26–28]. Structurally, hepsin is composed of 413 amino acids and has a C-terminal protease domain in the extracellular region [29]. Overexpression in advanced prostate cancer and the location of its active site at the cell surface make hepsin an attractive biomarker for imaging

* Corresponding authors.
E-mail addresses: sonsh0201@gmail.com (S.-H. Son), yjbyun1@korea.ac.kr (Y. Byun).
[1] Equal contribution.

https://doi.org/10.1016/j.bioorg.2019.102990
Received 22 February 2019; Received in revised form 16 May 2019; Accepted 17 May 2019
Available online 20 May 2019
0045-2068/

metastatic prostate cancer. High expression of hepsin has also been documented in several other cancers such as ovarian, breast, and renal cancer [30–33].

In the past decade, a number of low molecular weight (M. W.) hepsin ligands have been reported including peptide-derived analogs, benzamidines, and indolecarboxamidines [34–41]. Our group also reported dipeptide-derived hepsin inhibitors containing a Leu-Arg amino acid sequence [35]. Although several small molecules have been identified as potential inhibitors of hepsin, only a few of these are fluorescently labeled for selective and sensitive detection of prostate cancer [6,42].

We, herein, report the first hepsin-targeted NIR fluorescence imaging agents based on the structure of dipeptide-derived hepsin inhibitors. We previously published Leu-Arg hepsin ligands with strong affinity in the nanomolar K_i range [35]. For this purpose, we designed two NIR fluorescent hepsin ligands, one labeled with boron-dipyrromethene (BODIPY) and the other with SulfoCy7. The fluorophores are separated from the hepsin-binding moiety by a polyethyleneglycol (PEG) linker, in order to decrease both steric hindrance from the bulky fluorophore and the hydrophobicity of the conjugate compound.

2. Results and discussion

2.1. Design concept

$BODIPY_{650/665}$ and SulfoCy7 were chosen because they can be used for NIR optical imaging. In particular, $BODIPY_{650/665}$ was selected as a prosthetic group for hepsin conjugation because it has several advantages such as balance of hydrophilicity and hydrophobicity, sharp fluorescence peaks with high quantum yield, tolerance to a wide range of polarity and pH, and diverse chemical reactions for conjugating with targeting moieties or linkers [43–45]. In addition, the fluorine atom in the core structure of BODIPY can be exchanged with ^{18}F for PET imaging [46–49]. We previously reported that ketobenzothiazole (kbt) or ketothiazole (kt) analogs derived from Leu-Arg dipeptide exhibited strong hepsin inhibition [35]. In this work, we attached two NIR dyes to the dipeptide-derived hepsin inhibitors and evaluate their biological activities *in vitro* (Fig. 1).

2.2. Synthesis of novel $BODIPY_{650/665}$ activated ester

New $BODIPY_{650/665}$ fluorophore was synthesized as described in Scheme 1 by modifying the reported procedure [50]. Briefly, coupling of pyrrole-2-carboxaldehyde with 4-(bromomethyl)benzoic acid methyl ester *via* Wittig reaction afforded the alkene **3** in 23% yield. The *E*-isomer was obtained exclusively, which was confirmed by observing a coupling constant of 16.5 Hz in a ^1H NMR experiment. Compound **4** was prepared in 71% yield by reacting **3** with Vilsmeier reagent, which was generated from phosphoryl chloride and dimethylformamide in 1,2-dichloroethane. Bipyrrole **6** was prepared by adapting a reported procedure [51]. Condensation of **4** with **6** was achieved by treatment with phosphoryl chloride, followed by complexation with boron trifluoride, providing $BODIPY_{650/665}$ methyl ester **7** in 56% yield. Hydrolysis of compound **7** was performed by treating 4.5 N HCl solution in THF under reflux to afford the carboxylic acid **8**. Although several hydrolysis conditions including acid catalyst (HCl, H_3PO_4), acid concentration (1.0 to 5.0 N), solvent (THF, CH_2Cl_2), and reaction condition (rt, reflux) were explored, the best condition provided compound **8** in only 13% yield. The carboxylic acid **8** was converted into the activated ester **9** by reacting of **8** with *N*-hydroxysuccinimide (NHS) and 1-ethyl-3-(3-dimethylaminopropyl)carbodiimide hydrochloride (EDC·HCl) in dichloromethane. The appearance of a singlet peak at 2.93 ppm corresponding to the $–CH_2$ group of NHS in the ^1H NMR confirmed the formation of the NHS activated ester of $BODIPY_{650/665}$.

2.3. Synthesis of $BODIPY_{650/665}$-labeled hepsin ligand (1) and SulfoCy7-labeled hepsin ligand (2)

Leu-Arg-ketothiazole (Leu-Arg-kt) hepsin ligand conjugated with PEG linker was synthesized as shown in Scheme 2. The target compound **15** was prepared from compound **10** in 5 synthetic steps. Initially, we attempted to conjugate **10** with Leu-Arg-kt ligand by using peptide coupling conditions (e.g., HATU as coupling reagent, DIPEA as base, DMF as solvent, room temperature), however, failed in obtaining the desired product. Therefore, we carried out the conjugation of Leu with PEG linker, followed by peptide coupling between Leu and Arg-kt. Compound **12** was obtained in 71% yield by using EDC·HCl, 1-hydroxybenzotriazole (HOBt). Hydrolysis of **12** with 25% trifluoroacetic acid (TFA) solution in dichloromethane afforded compound **13**. Coupling of **13** with H_2N-Arg(Mtr)-kt provided compound **14** in 55% yield. Global deprotection of **14** was successfully achieved in 57% yield to afford compound **15** by a two-step procedure. The Mtr-protecting groups were removed by the treatment of strong acid (95% TFA), followed by the deprotection of Fmoc group using 20% piperidine in THF. Temperature was one of the key factors that contributed to the high yield of this step. The cyclized by-product was obtained upon heating while concentrating under reduced pressure (See supporting information).

The BODIPY-labeled ligand **1** and the SulfoCy7-labeled ligand **2** were synthesized by conjugating compound **15** with $BODIPY_{650/665}$ NHS ester (**9**) or commercial SulfoCy7 NHS ester, respectively. The coupling reaction was carried out at room temperature for 16 h in the presence of triethylamine as a base. The final compounds were purified by reversed-phase (RP)-HPLC using a linear gradient of acetonitrile and

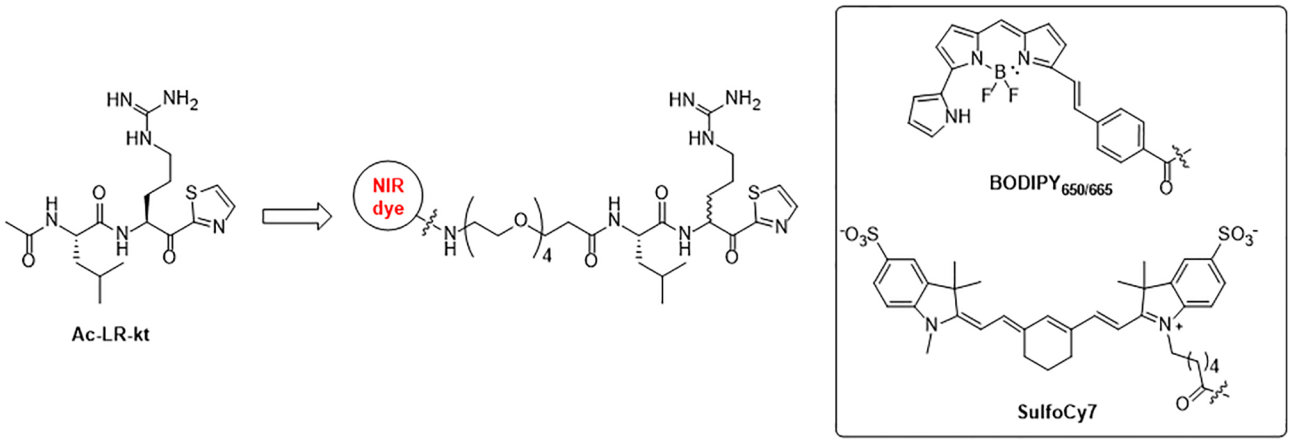

Fig. 1. Design of hepsin-targeted optical imaging probes based on Ac-LR-kt, the known hepsin inhibitor.

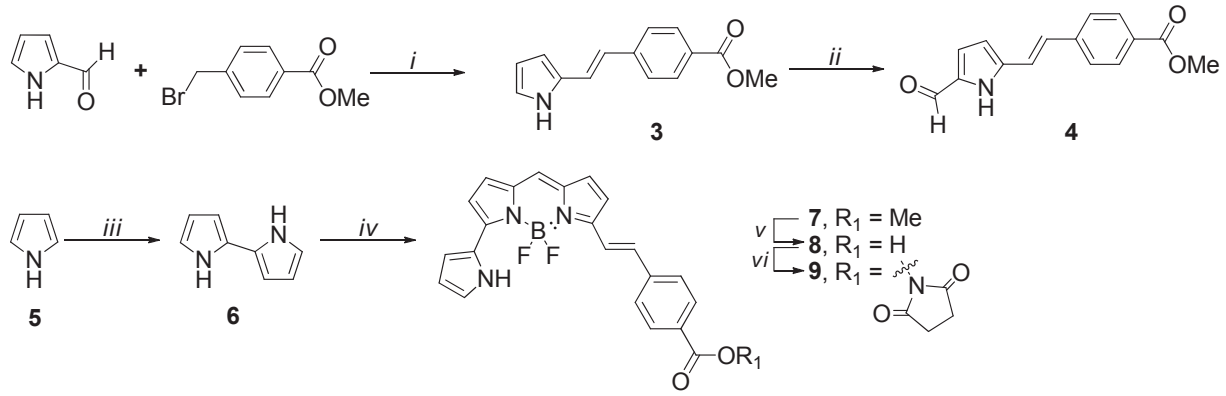

Scheme 1. Synthesis of novel $BODIPY_{650/665}$ activated ester. [a]Reagents and reaction conditions: (*i*) PBu_3, Zn, 100 °C, 15 h, benzene, 23%; (*ii*) DMF, $POCl_3$, reflux, 15 min, CH_2Cl_2 then NaOAc, 71%; (*iii*) PIFA, TMSBr, −78 °C, 1 h, CH_2Cl_2, 65%; (*iv*) compound **4**, $POCl_3$, rt, 5.5 h, CH_2Cl_2 then DIPEA, $BF_3{\cdot}Et_2O$, 2 h, 56%; (*v*) 4.5 N HCl/THF (1/4, v/v), reflux, 18 h, 13%; (*vi*) EDC·HCl, *N*-hydroxysuccinimide, CH_2Cl_2, rt, 2 h.

water containing 0.1% formic acid. The purities of the final compounds were assessed using RP-HPLC. As shown in the RP-HPLC chromatograms of compounds **1**–**2** (see supporting information), the BODIPY-attached hepsin ligand **1** (Rt: 9.45 min) was more hydrophobic than the corresponding SulfoCy7 ligand **2** (Rt: 3.86 min).

2.4. In vitro biological evaluation

The hepsin inhibitory activities of the conjugates **1**–**2** were determined by a fluorescence-based enzymatic assay, which uses Boc-QAR-AMC as a substrate and recombinant human hepsin as an enzyme.

Table 1
Enzyme activity of the synthesized compounds against hepsin and matriptase.

Compound	Hepsin K_i (nM)[a]	Matriptase K_i (nM)[a]	Hepsin selectivity
Ac-LR-kt	22.4 ± 0.50	334 ± 62	14.9
1	20.9 ± 1.54	> 30,000	> 1000
2	22.1 ± 1.37	> 30,000	> 1000
15	42.3 ± 3.23	134 ± 34	3.2
18	6.45 ± 0.44	403 ± 32	62.5

[a] Measurements of enzymatic activity were performed in triplicate and represent the mean ± SD at least three experiment sets.

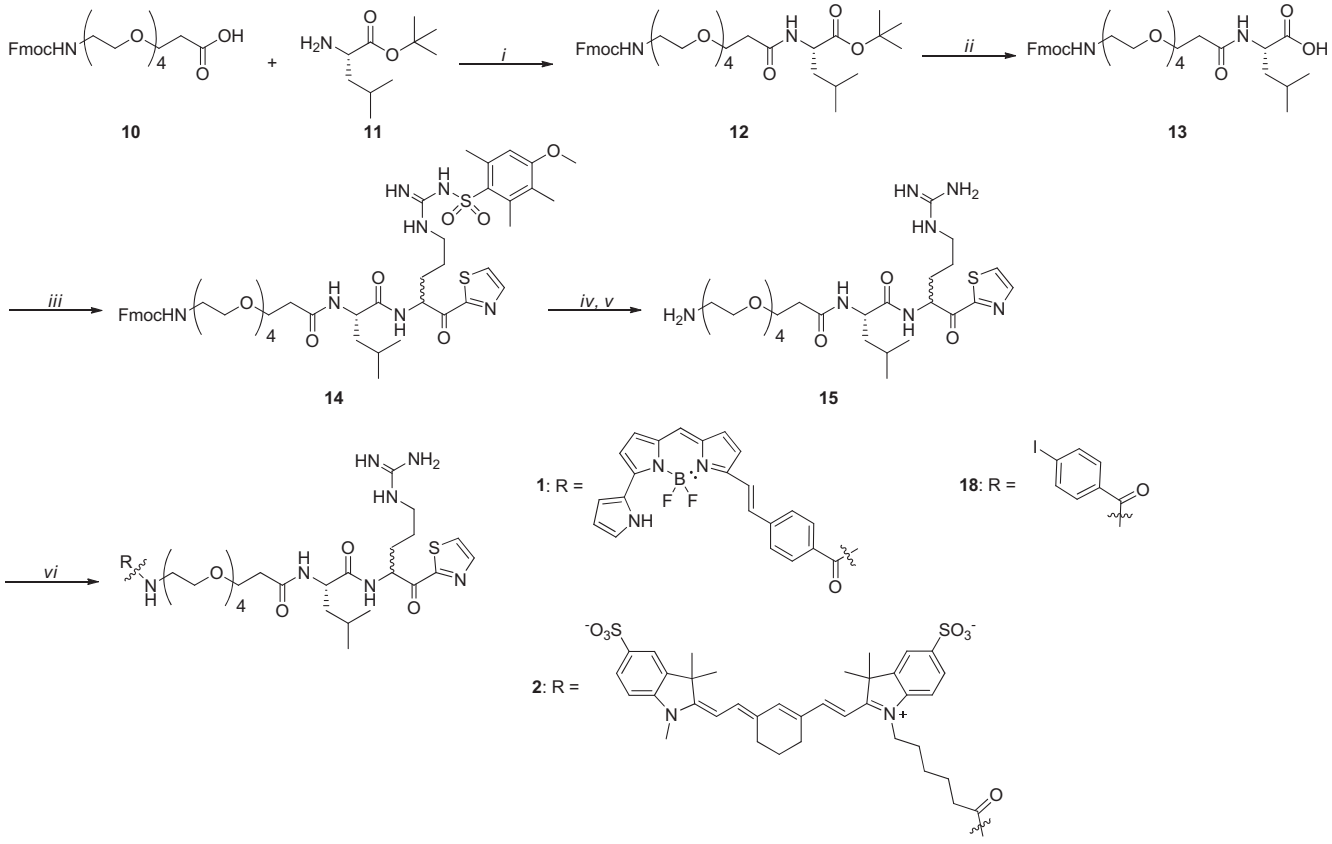

Scheme 2. Synthesis of $BODIPY_{650/665}$-labeled ligand **1** and SulfoCy7-labeled ligand **2.** [a]Reagents and reaction conditions: (*i*) HOBt, EDC·HCl, THF, 0 °C to rt, 12 h, 71%; (*ii*) 25% TFA in CH_2Cl_2, 0 °C to rt, 5 h, quantitative; (*iii*) NH_2Arg(Mtr)-kt, HOBt, EDC·HCl, THF, 0 °C to rt, 12 h, 55%; (*iv*) TFA/thioanisole/water (95/2.5/2.5 (v/v/v)), rt, 3 h; (*v*) 20% piperidine in THF, 0 °C, 10 min, 57% in two steps; (*vi*) compound **9** (for **1**), sulfoCy7 NHS ester (for **2**), or 4-iodobenzoic acid NHS ester (for **18**), Et_3N, DMF, rt, 16 h (for **1** and **2**) or 5 h (for **18**), 84% (for **1**), 50% (for **2**), 63% (for **18**).

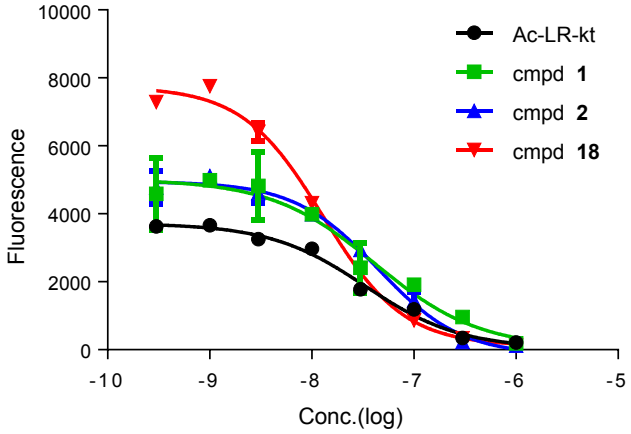

Fig. 2. IC_{50} curves of compounds **1, 2, 18** and **Ac-LR-kt.**

Ac-LR-kt and the hepsin ligand (**15**) without attaching an optical dye were included as positive controls for comparison. The results of the hepsin assay are summarized in Table 1. New hepsin-targeted optical probes showed strong hepsin-inhibitory activities (20.9 nM for **1** and 22.1 nM for **2**), which were more potent than compound **15** (42.3 nM). The other positive control Ac-LR-kt (22.4 nM) showed similar hepsin affinity with the bulky compounds **1–2**. Two diastereomers of compound **2** were separated by HPLC and their K_i values were determined (see supporting information). The diastereomer at 4.20 min in the HPLC chromatogram of **2** inhibited hepsin much stronger than one at 3.86 min. Compound **18** with an iodobenzoyl moiety inhibited hepsin stronger than compounds **1–2** with a K_i value of 6.45 nM (Fig. 2). However, both **1** and **2** showed increased selectivity for hepsin over matriptase compared with **18** (> 1000-fold for **1–2** vs. 62-fold for **18**). To our knowledge, this is the first report of hepsin-targeted imaging probes that possess K_i values in the range of 20 nM with high selectivity for hepsin over matriptase (see Table 1).

2.5. In vitro cell uptake studies

We evaluated the hydrophilic hepsin-SulfoCy7 ligand **2** for its ability to bind to hepsin on a surface of prostate cancer cells. Flow cytometric analyses of the ligand **2** exhibited dose-dependent binding to hepsin-expressing PC3/ML/Hepsin cells. However, it did not bind to the non-hepsin-expressing cell PC3/ML cells, indicating that the binding of compound **2** is specific to hepsin (Fig. 3). These data are consistent with strong hepsin-binding affinity of the ligand **2**. However, the hepsin-BODIPY ligand **1** had non-specific accumulation in both cells despite its strong binding for hepsin at the enzyme assay. It might be due to the hydrophobic BODIPY nature of **1**.

2.6. Molecular modeling studies

We performed molecular docking studies of compounds **1–2** with the hepsin X-ray crystal structure (PDB ID: 1O5E) by using *Surflex-Dock GeomX* module of Sybyl software [52] to elucidate their binding mode at the active site of hepsin. The common dipeptide region (Leu-Arg) of **1–2** made strong hydrogen-bonding interactions with Asp189 and Gly219 (Fig. 4), which are key amino acid residues to interact with the amidine region of 6-halo-5-amidinoindole and 6-halo-5-amidinobenzimidazole hepsin inhibitors [52]. The difference between **1** and **2** was the orientation of the bulky optical dye scaffold. While the BODIPY moiety of **1** was located close to the surface of hepsin, the SulfoCy7 region of **2** was projected toward water environment. Although the orientation of the NIR dye region was so different, hepsin-binding affinities of both compounds was almost similar, indicating that hydrogen-bonding contacts with Asp189 and Gly219 are essential for binding to hepsin.

3. Conclusion

We have designed and synthesized new hepsin-targeted inhibitors conjugated with NIR optical imaging dyes. The Leu-Arg-kt analogs labeled with BODIPY (**1**) or SulfoCy7 (**2**) exhibited strong *in vitro* hepsin-inhibitory activities with K_i values of 20 nM range and high selectivity for hepsin over matriptase. Cell uptake studies of **2** exhibited selective targeting and retention in hepsin-overexpressing cells. Compound **2** has the potential to be utilized for the discovery and development of hepsin-targeted imaging probes and provides valuable information for rational design of novel hepsin inhibitors.

4. Experimental section

4.1. General methods

All the chemicals and solvents used in the reaction were purchased from Sigma-Aldrich, TCI, or Alfa Aesar, and were used without further purification. Reactions were monitored by TLC on 0.25 mm Merck precoated silica gel plates (60 F_{254}). Reaction progress was monitored by TLC analysis using a UV lamp. Column chromatography was performed on silica gel (230–400 mesh, Merck, Darmstadt, Germany). NMR spectra were recorded at room temperature on either Bruker BioSpin Avance 300 MHz NMR or Bruker Ultrashield 600 MHz Plus spectrometer. Chemical shifts are reported in parts per million (ppm, δ) with TMS as an internal standard. Coupling constant are given in Hertz. ^{13}C NMR spectra were obtained by using the same NMR spectrometers and were calibrated with $CDCl_3$ (δ = 77.16 ppm). Splitting patterns are indicated as s, singlet; d, doublet; t, triplet; q, quartet; m, multiplet; br, broad for ^1H NMR data. High resolution mass spectra (HRMS) were recorded on an Agilent 6530 Accurate mass Q-TOF LC/MS spectrometer. Low resolution mass spectra (LRMS) analyses were obtained from a API 150EX ESI-MS spectrometer. High-performance liquid chromatography purification was performed on Agilent 1260 Infinity (Agilent) or Shimadzu system (system controller CMB-20A, two pumps LC-20AR, photodiode array detector SPD-20AV).

The purity of all final compounds was measured by analytical reversed-phase high-performance liquid chromatography(RP-HPLC) on an Agilent 1260 Infinity (Agilent) with a C18 column (Phenomenex, 150 × 4.6 mm, 3 μm, 110 Å). RP-HPLC was performed using an isocratic elution (method A) or a linear gradient elution (method B). The isocratic elution was mobile phase consisting of acetonitrile–water (35:65, v/v) with 0.1% formic acid (FA). The gradient elution process included 10% to 90% of solvent B over 20 min (A = 0.1% FA in water and B = 0.1% FA in acetonitrile). All compounds were eluted with a flow rate of 1.0 mL/min and monitored at UV detector: 254 nm, 650 nm (for $BODIPY_{660/665}$- labeled compound), and 773 nm (for SulfoCy7-labeled compound). Purity of the tested compounds was > 95%.

4.2. Preparation of novel $BODIPY_{650/665}$ NHS ester (9)

4.2.1. (E)-Methyl 4-(2-(1H-pyrrol-2-yl)vinyl)benzoate (3)

To a solution of methyl 4-bromomethylbenzoate (4.8 g, 21.0 mmol), tributylphosphine (5.2 mL, 21.0 mmol) and zinc (1.4 g, 21.0 mmol) in benzene was added pyrrole-2-carboxaldehyde (2.0 g, 21.0 mmol). The reaction mixture was stirred at 100 °C for 15 h. After cooling to room temperature, the reaction mixture was diluted with CH_2Cl_2 (100 mL). The organic layer was washed with water (50 mL × 3). The organic layer was dried over $MgSO_4$, filtered, and concentrated under reduced pressure. The crude residue was purified by silica gel column chromatography (toluene:EtOAc = 50:1 to 40:1, v/v) to afford compound **3** (1.1 g, 23%) as a yellow solid. R_f = 0.64 (toluene:EtOAc = 5:1, v/v). ^1H NMR (300 MHz, $CDCl_3$) δ 8.41 (brs, 1H), 7.99 (d, J = 8.4 Hz, 2H), 7.47 (d, J = 8.4 Hz, 2H), 7.09 (d, J = 16.5 Hz, 1H), 6.86 (d, J = 0.9 Hz, 1H),

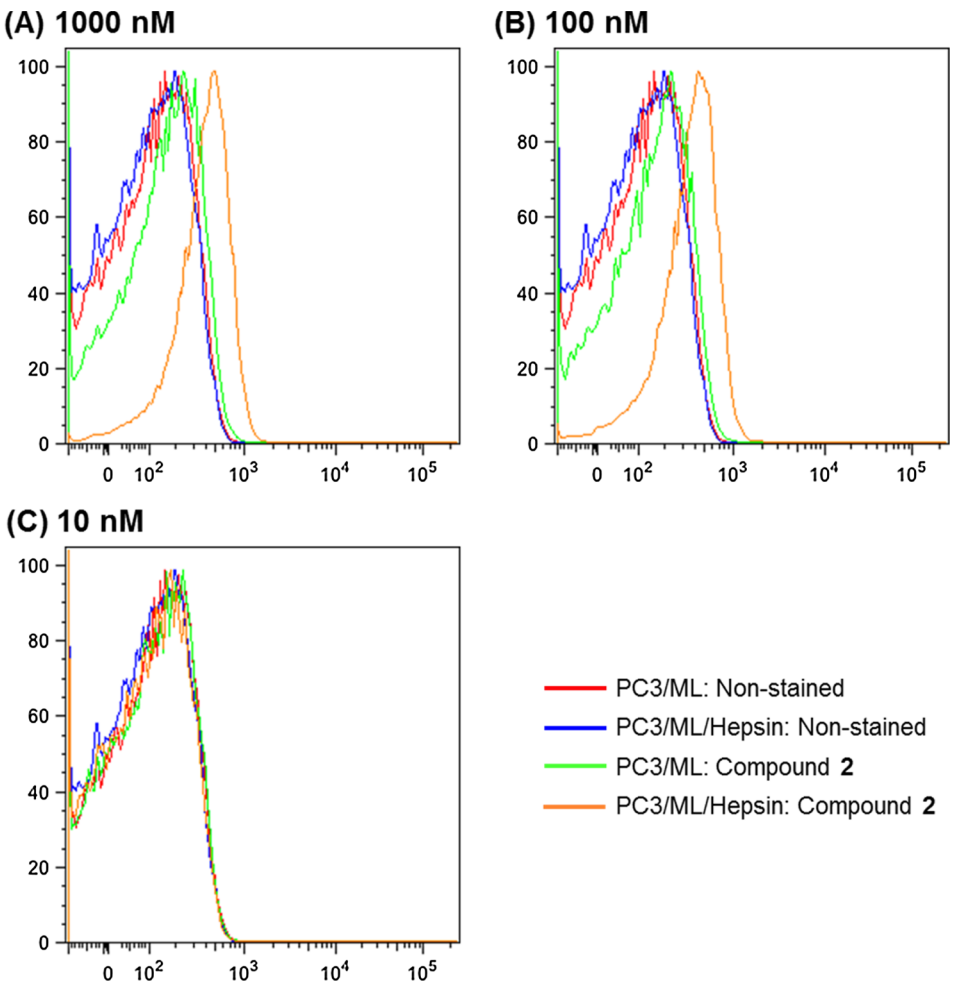

Fig. 3. *In vitro* uptake study of compound **2** in PC3/ML and PC3/ML/Hepsin cell lines.

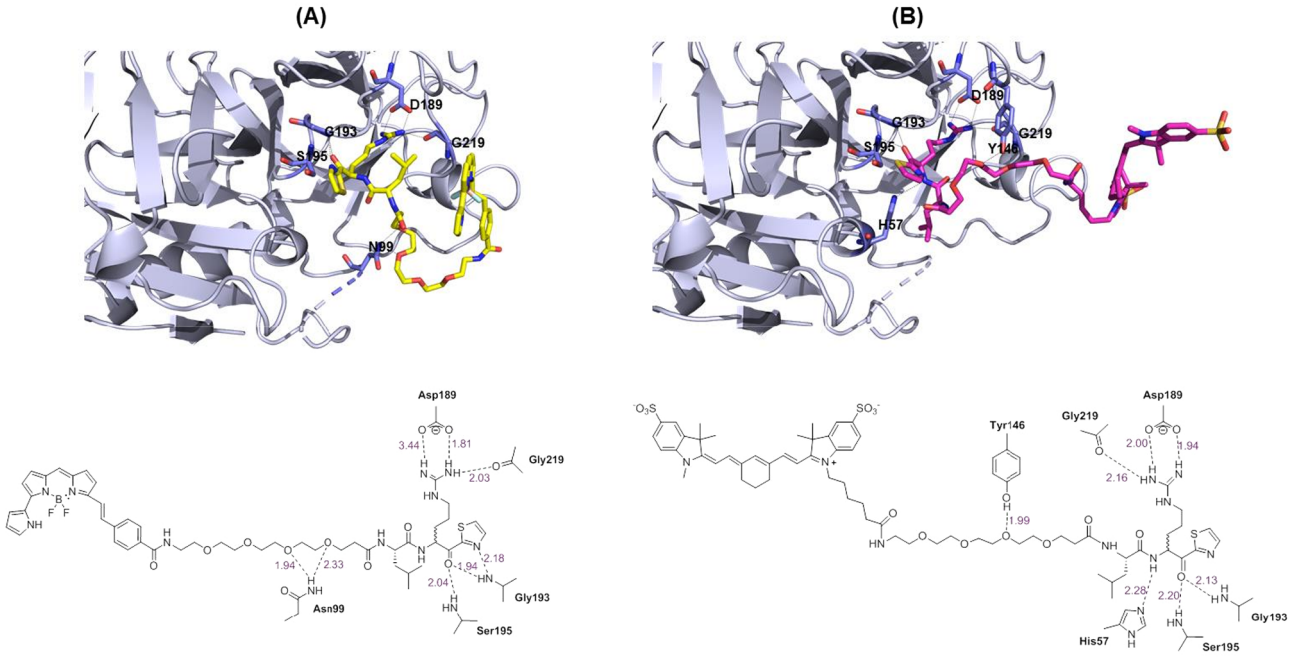

Fig. 4. Docked poses of hepsin-targeted optical probes (**A**: compound **1**, **B**: compound **2**) at the active site of hepsin.

6.67 (d, J = 16.5 Hz, 1H), 6.42 (brs, 1H), 6.27 (dd, J = 2.4 and 5.9 Hz, 1H), 3.91 (s, 3H); ^{13}C NMR (75 MHz, $CDCl_3$) δ 166.9, 142.1, 130.4, 130.1, 128.2, 125.5, 122.0, 121.3, 119.9, 110.4, 110.3, 52.0. LRMS (ESI) m/z 226.4 $[M-H]^-$.

4.2.2. (E)-Methyl 4-(2-(5-formyl-1H-pyrrol-2-yl)vinyl)benzoate (4)

Phosphorus oxychloride (92 μL, 0.99 mmol) was added dropwise to anhydrous DMF (76 μL, 0.99 mmol) at 0 °C. The solution was warmed to room temperature and stirred for 15 min. The mixture was cooled to 0 °C and diluted with anhydrous 1,2-dichloroethane (10 mL). A solution of **3** (200 mg, 0.88 mmol) in anhydrous 1,2-dichloroethane (15 mL) was added dropwise to the solution. The reaction mixture was stirred under reflux for 1 h. The reaction mixture was cooled to room temperature and quenched with a solution of sodium acetate trihydrate (1.3 g, 9.9 mmol) in water (5 mL). The reaction mixture was stirred under reflux for 1 h. The organic layer was collected and the aqueous layer extracted with CH_2Cl_2. The combined organic layer was washed with saturated aqueous $NaHCO_3$ solution, dried over $MgSO_4$, and concentrated under reduced pressure. The crude residue was purified by silica gel column chromatography (toluene:EtOAc = 40:1 to 5:1, v/v) to give compound **4** (160 mg, 71%) as a yellow solid. R_f = 0.33 (toluene:EtOAc = 5:1, v/v). ^{1}H NMR (300 MHz, $CDCl_3$) δ 10.24 (brs, 1H), 9.52 (s, 1H), 8.03 (d, J = 8.4 Hz, 2H), 7.54 (d, J = 8.4 Hz, 2H), 7.17 (d, J = 16.5 Hz, 1H), 7.10 (d, J = 16.5 Hz, 1H), 7.01 (dd, J = 2.4 and 3.9 Hz, 1H), 6.54 (dd, J = 2.4 and 8.0 Hz, 1H), 3.93 (s, 3H); ^{13}C NMR (75 MHz, $CDCl_3$) δ 179.0, 166.9, 141.0, 138.6, 133.4, 130.3, 129.6, 129.6, 126.4, 123.1, 119.8, 111.6, 52.3.

4.2.3. 1H,1′H-2,2′-Bipyrrole (6)

To a solution of 1*H*-pyrrole **5** (187 μL, 2.7 mmol) in CH_2Cl_2 (15 mL) were added PIFA(387 mg, 0.9 mmol) and TMSBr (233 μL, 1.8 mmol) at −78 °C. The reaction mixture was stirred at the same temperature for 1 h. After the reaction was completed, saturated aqueous $NaHCO_3$ solution (ca. 50 mL) was added to the reaction mixture. The reaction mixture was stirred for an additional 10 min at ambient temperature. The organic layer was separated and the water layer was washed with CH_2Cl_2. The combined organic layer was dried with $MgSO_4$, filtered, and concentrated. The crude residue was purified by silica gel column chromatography (toluene:EtOAc = 40:1 to 5:1, v/v) to give compound **6** (116 mg, 65%) as a colorless oil. R_f = 0.32 (hexane:EtOAc = 4:1, v/v). ^{1}H NMR (300 MHz, $CDCl_3$) δ 8.22 (brs, 2H), 6.79–6.74(m, 2H), 6.27–6.19 (m, 4H). LRMS (ESI) m/z calcd for $C_8H_8N_2[M+H]^+$, 133.1; found, 133.0. ^{1}H NMR and MS data were in complete agreement with those previously reported [51].

4.2.4. Methyl 4-((E)-2-((Z)-2-((1-(difluoroboryl)-1H,1′H-[2,2′-bipyrrol]-5-yl)methylene)-2H-pyrrol-5-yl)vinyl)benzoate (7)

The reaction was carried out in the dark. To a solution of **4** (260 mg, 1.02 mmol) and **6** (134 mg, 1.02 mmol) in anhydrous CH_2Cl_2 (20 mL) was added phosphorus oxychloride (142 μL, 1.53 mmol). The reaction mixture was stirred for 15 h. After the excess solvent was evaporated, the remaining residue was dissolved in anhydrous CH_2Cl_2 (20 mL). *N,N*-Diisopropylethylamine (1.7 mL, 10.2 mmol) and $BF_3{\cdot}OEt_2$ (2.9 mL, 10.2 mmol) were added slowly to the solution. The mixture solution was stirred for 3 h. The reaction mixture was washed with brine, dried over $MgSO_4$, filtered, and concentrated under reduced pressure. The crude residue was purified by silica column chromatography (hexane:EtOAc = 2:1, v/v) to afford compound **7** (240 mg, 56%) as blue solid. R_f = 0.31 (hexane:EtOAc = 2:1, v/v). ^{1}H NMR (300 MHz, $CDCl_3$) δ 10.50 (brs, 1H), 8.06 (d, J = 8.4 Hz, 2H), 7.73 (d, J = 16.5 Hz, 1H), 7.66 (d, J = 8.4 Hz, 2H), 7.31–7.22 (m, 2H),7.07 (d, J = 4.8 Hz, 1H), 7.03 (brs, 1H), 6.98 (s, 1H), 6.95–6.89 (m, 3H), 6.43–6.40 (m, 1H), 3.94 (s, 3H); ^{13}C NMR (75 MHz, $CDCl_3$) δ 166.9, 150.6, 150.3, 141.3, 138.3, 135.4, 132.9, 131.5, 130.2, 129.7, 127.1, 126.4, 126.3, 124.0, 121.70, 121.0, 118.4, 115.4, 111.9, 52.3. HRMS (ESI): calcd for $C_{23}H_{18}BF_2N_3O_2[M-H]^-$, 416.1387; found, 416.1389.

4.2.5. 4-((E)-2-((Z)-2-((1-(Difluoroboryl)-1H,1′H-[2,2′-bipyrrol]-5-yl)methylene)-2H-pyrrol-5-yl)vinyl)benzoic acid (8)

The reaction was carried out in the dark. To a solution of **7** (400 mg, 0.96 mmol) in THF (40 mL) was added aqueous HCl solution (4.5 M, 10 mL). The reaction mixture was stirred under reflux for 18 h. The solution was cooled to room temperature, diluted with water (ca. 50 mL), and washed with EtOAc. The combined organic layer was dried over $MgSO_4$, filtered, and concentrated under reduced pressure. The crude residue was purified by silica gel column chromatography (CH_2Cl_2:MeOH = 30:1 to 10:1, v/v) to afford compound **8** (52 mg, 13%) as a dark blue solid. R_f = 0.33 (CH_2Cl_2:MeOH = 10:1, v/v). ^{1}H NMR (300 MHz, CD_3OD) δ 8.05 (d, J = 8.4 Hz, 2H), 7.77 (d, J = 16.5 Hz, 1H), 7.70 (d, J = 8.4 Hz, 2H), 7.41 (d, J = 16.2 Hz, 1H), 7.29 (dd, J = 1.2 and 2.4 Hz, 1H), 7.25 (dd, J = 1.5 and 3.9 Hz, 1H), 7.23 (s, 1H), 7.22 (d, J = 4.5 Hz, 1H), 7.07 (d, J = 4.5 Hz, 1H), 7.04 (d, J = 4.2 Hz, 1H), 7.00 (d, J = 4.2 Hz, 1H), 6.40 (dd, J = 2.7 and 3.9 Hz, 1H). HRMS (ESI): calcd for $C_{22}H_{16}BF_2N_3O_2[M-H]^-$, 402.1231; found, 402.1231. > 95% purity (as determined by RP-HPLC, method B, retention time = 16.84 min).

4.2.6. 2,5-Dioxopyrrolidin-1-yl 4-((E)-2-((Z)-2-((1-(difluoroboryl)-1H,1′H-[2,2′-bipyrrol]-5-yl)methylene)-2H-pyrrol-5-yl)vinyl)benzoate (9)

To a solution of compound **8** (25 mg, 62 μmol) in dry dichloromethane (20 mL) was added *N*-hydroxysuccinimide (29 mg, 0.25 mmol) and EDC·HCl (48 mmol). The reaction mixture was stirred at room temperature for 4 h and was quenched with cooled HCl solution (1.0 M, ca. 20 mL). The solution was with iced water and extracted with CH_2Cl_2 (ca. 20 mL twice). The combined organic layer was washed with brine, dried over $MgSO_4$, filtered, and concentrated under reduced pressure to afford compound **9** (28 mg, 90%). The product was used in the next step without further purification. R_f = 0.78 (hexane:EtOAc = 1:1, v/v). ^{1}H NMR (300 MHz, $CDCl_3$) δ 10.51 (brs, 1H), 8.14 (d, J = 8.4 Hz, 2H), 7.78 (d, J = 16.5 Hz, 1H), 7.71 (d, J = 8.4 Hz, 2H), 7.29–7.21 (m, 2H), 7.08 (d, J = 4.8 Hz, 1H), 7.05 (brs, 1H), 6.98 (s, 1H), 6.95–6.90 (m, 3H), 6.42 (brs, 1H), 2.93 (s, 4H). HRMS (ESI): calcd for $C_{26}H_{19}BF_2N_4O_4[M-H]^-$, 499.1394; found, 499.1378. > 95% purity (as determined by RP-HPLC, method B, retention time = 11.20 min).

4.3. Preparation of compound 15

4.3.1. (S)-tert-Butyl 1-(9H-fluoren-9-yl)-21-isobutyl-3,19-dioxo-2,7,10,13,16-pentaoxa-4,20-diazadocosan-22-oate (12)

To a solution of compound **10** (785 mg, 1.6 mmol) and L-leucine *tert*-butyl ester hydrochloride **11** (291 mg, 1.3 mmol) in THF (10 mL) were added HOBt (281 mg, 2.08 mmol) and EDC·HCl (399 mg, 2.08 mmol) at 0 °C. The reaction mixture was stirred at room temperature overnight. The reaction mixture was quenched with saturated aqueous $NaHCO_3$ solution (ca. 10 mL) and extracted with EtOAc (ca. 150 mL). The combined organic layer was washed with brine, dried over $MgSO_4$, filtered, and concentrated *in vacuo*. The crude residue was purified by silica gel column chromatography (CH_2Cl_2:MeOH = 60:1 to 50:1, v/v) to give compound **12** (604 mg, 71%) as a colorless oil. R_f = 0.64 (CH_2Cl_2:MeOH = 10:1, v/v). ^{1}H NMR (300 MHz, $CDCl_3$) δ 7.76 (d, J = 7.5 Hz, 2H), 7.60 (d, J = 7.5 Hz, 2H), 7.40 (t, J = 7.2 Hz, 2H), 7.31 (t, J = 7.5 Hz, 2H), 6.59 (d, J = 7.8 Hz, 1H), 5.42 (brs, 1H), 4.54–4.45 (m, 1H), 4.40 (d, J = 6.9 Hz, 2H), 4.22 (t, J = 6.6 Hz, 1H), 3.71 (t, J = 5.7 Hz, 1H), 3.69–3.53 (m, 15H), 3.45–3.34 (m, 2H), 2.48 (t, J = 5.7 Hz, 2H), 1.73–1.42 (m, 3H), 1.45 (s, 9H), 0.93 (d, J = 6.3 Hz, 6H); ^{13}C NMR (75 MHz, $CDCl_3$) δ 171.9, 170.9, 156.3, 143.6, 140.9, 127.3, 126.7, 124.7, 119.5, 81.0, 70.1, 70.0, 69.9, 69.8, 69.8, 66.8, 66.1, 50.9, 49.7, 46.8, 41.1, 40.5, 36.3, 27.6, 24.5, 22.5, 21.7. HRMS (ESI): calcd for $C_{36}H_{52}N_2O_9[M+Na]^+$, 679.3565; found, 679.3568.

*4.3.2. (S)-1-(9H-Fluoren-9-yl)-21-isobutyl-3,19-dioxo-2,7,10,13,16-pentaoxa-4,20-diazadocosan-22-oic acid (**13**)*

To a solution of **12** (200 mg, 0.3 mmol) in CH_2Cl_2 (7.5 mL) was added slowly trifluoroacetic acid (2.5 mL) at 0 °C. The reaction mixture was stirred at room temperature for 5 h. The reaction mixture was diluted with CH_2Cl_2 and poured into iced water. The organic layer was washed with saturated aqueous $NaHCO_3$ solution, followed by brine. The combined organic phase was dried over $MgSO_4$ and concentrated under reduced pressure to give compound **13** (192 mg, quantitative) as colorless oil. R_f = 0.31 (CH_2Cl_2:MeOH = 10:1, v/v). ^{1}H NMR (300 MHz, $CDCl_3$) δ 9.24 (brs, 1H), 7.75 (d, J = 7.5 Hz, 2H), 7.60 (d, J = 7.5 Hz, 2H), 7.39 (t, J = 7.2 Hz, 2H), 7.33 (t, J = 7.5 Hz, 2H), 7.02 (d, J = 7.8 Hz, 1H), 5.63 (brs, 1H), 4.68–4.52 (m, 1H), 4.39 (d, J = 6.9 Hz, 2H), 4.29–4.13 (m, 1H), 3.78–3.51 (m, 16H), 3.47–3.32 (m, 2H), 2.57–2.43 (m, 2H), 1.78–1.52 (m, 3H), 0.93 (d, J = 5.4 Hz, 6H); ^{13}C NMR (75 MHz, $CDCl_3$) δ 174.8, 172.2, 156.8, 144.0, 141.3, 127.7, 127.1, 125.6, 125.1, 120.0, 68.0, 67.1, 66.7, 50.9, 47.2, 41.2, 40.9, 36.6, 25.6, 24.9, 23.0, 22.0. HRMS (ESI): calcd for $C_{32}H_{44}N_2O_9$ [M + Na]$^+$, 623.2939; found, 623.2940.

*4.3.3. (9H-Fluoren-9-yl)methyl ((9S)-1-imino-9-isobutyl-1-(4-methoxy-2,3,6-trimethylphenylsulfonamido)-8,11-dioxo-6-(thiazole-2-carbonyl)-14,17,20,23-tetraoxa-2,7,10-triazapentacosan-25-yl)carbamate (**14**)*

To a solution of **13** (384 mg, 0.64 mmol) and *N*-(*N*-(4-amino-5-oxo-5-(thiazol-2-yl)pentyl)carbamimidoyl)-4-methoxy-2,3,6-trimethylbenzenesulfonamide (233 mg, 0.51 mmol) in THF (5 mL) were added HOBt (108 mg, 0.8 mmol) and EDC·HCl (154 mg, 0.8 mmol) at 0 °C. The reaction mixture was allowed to slowly warm to room temperature and stirred overnight at room temperature. The reaction mixture was quenched with saturated aqueous $NaHCO_3$ solution (ca. 10 mL) and extracted with EtOAc. The combined organic layer was washed with brine, dried over $MgSO_4$, and concentrated *in vacuo*. The crude residue was purified by silica gel column chromatography (CH_2Cl_2:MeOH = 30:1 to 10:1, v/v) to give compound **14** (290 mg, 55%) as colorless oil. R_f = 0.51 (CH_2Cl_2:MeOH = 10:1, v/v). ^{1}H NMR (300 MHz, $CDCl_3$) δ 7.99 (d, J = 3.0 Hz, 1H), 7.75 (d, J = 7.5 Hz, 2H), 7.71–7.67 (m, 1H), 7.59 (t, J = 7.2 Hz, 2H), 7.38 (t, J = 7.5 Hz, 2H), 7.30 (d, J = 7.5 Hz, 2H), 6.49 (s, 1H), 6.36 (s, 2H), 5.63–5.51 (m, 1H), 4.54–4.38 (m, 1H), 4.38 (d, J = 6.9 Hz, 2H), 4.20 (t, J = 6.6 Hz, 1H), 3.79 (s, 3H), 3.69–3.53 (m, 15H), 3.52–3.11 (m, 4H), 2.68 (s, 3H), 2.59 (s, 3H), 2.62–2.41 (m, 1H), 2.10 (s, 3H), 2.20–2.03 (m, 1H), 1.81–1.42 (m, 6H), 0.88 (dd, J = 5.4 and 13.1 Hz, 6H); ^{13}C NMR (75 MHz, $CDCl_3$) δ 191.0, 172.3, 164.3, 158.2, 156.3, 156.4, 156.4, 145.3, 145.2, 144.0, 141.3, 138.5, 136.4, 134.0, 127.7, 127.1, 125.1, 124.6, 120.0, 111.6, 70.4, 70.3, 70.2, 70.1, 70.0, 67.0, 66.6, 55.4, 50.5, 47.2, 40.9, 40.4, 40.3, 25.3, 24.8, 24.7, 24.1, 23.1, 23.0, 21.8, 18.4, 12.0. HRMS (ESI): calcd for $C_{51}H_{69}N_7O_{12}S_2$[M + H]$^+$, 1036.4518; found, 1036.4519.

*4.3.4. 1-Amino-N-((2S)-1-((5-guanidino-1-oxo-1-(thiazol-2-yl)pentan-2-yl)amino)-4-methyl-1-oxopentan-2-yl)-3,6,9,12-tetraoxapentadecan-15-amide (**15**)*

Compound **14** (104 mg, 0.1 mmol) was dissolved in TFA/thioanisole/water (95/2.5/2.5, v/v/v, 3 mL) and the solution was stirred vigorously for 3 h. The reaction mixture was quenched with iced water and concentrated under reduced pressure at 4 °C. The crude residue was filtrated through a pad of silica gel (CH_2Cl_2:MeOH = 10:1, v/v) and the filtrate was concentrated under reduced pressure.

To a solution of the intermediate in THF (4 mL) was added dropwise piperidine (1 mL) at 0 °C. The reaction mixture was stirred vigorously for 10 min. The reaction mixture was quenched with iced water and concentrated under reduced pressure at 4 °C. The crude residue was treated with cold diethyl ether (40 mL) and the ether layer was decanted. The crude residue was dissolved with a mixture of water and acetonitrile (1:1, 0.1% formic acid), filtered through a 0.45 μm PTFE filter, and purified by semi-preparative RP-HPLC (using conditions: column, Phenomenex Gemini-NX C18, 110 Å, 150 mm × 10 mm, 5 μm; flow rate, 2 mL/min; mobile phase, A = 0.1% formic acid (FA) in water and B = 0.1% FA in acetonitrile; gradient, 5% B to 90% B over 20 min; detection, 220 nm and 254 nm) to give compound **15** (retention time = 7.48 and 7.83 min) in 57% yield. ^{1}H NMR (300 MHz, CD_3CN–D_2O = 1:1, v/v) δ 8.06 (dd, J = 0.9 and 3.0 Hz, 1H), 7.99 (dd, J = 0.9 and 3.0 Hz, 1H), 5.42–5.33 (m, 1H), 4.33–4.27 (m, 1H), 3.73–3.42 (m, 16H), 3.19–2.97 (m, 4H), 2.54–1.83 (m, 2H), 2.13–1.89 (m, 1H), 1.87–1.38 (m, 1H), 0.83 (dd, J = 6.3 and 13.2 Hz, 6H); ^{13}C NMR (75 MHz, CD_3CN–D_2O = 1:1, v/v) δ 192.6, 192.5, 174.9, 174.3, 174.2, 165.1, 157.6, 146.2, 129.6, 129.6, 70.5, 70.4, 67.6, 67.2, 55.8, 55.7, 53.1, 53.0, 41.4, 41.6, 40.0, 36.8, 36.7, 28.7, 28.6, 25.5, 25.5, 25.3, 25.2, 23.1, 21.9, 21.8. HRMS (ESI): calcd for $C_{26}H_{47}N_7O_7S$[M + H]$^+$, 601.3258; found, 602.3344.

*4.4. Preparation of BODIPY$_{650/665}$-labeled hepsin ligand (**1**)*

To a mixture of **9** (2.40 mg, 4.80 μmol) and **15** (1.72 mg, 2.86 μmol) in DMF (1 mL) was added triethylamine (25 μL, 180 μmol). The reaction mixture was stirred at room temperature for 16 h. The reaction mixture was quenched with a mixture of acetonitrile (ACN) and water (1:1, 0.1% formic acid, 1 mL), and filtered through a 0.45 μm PTFE filter. The filtrate was purified by RP-HPLC as described for compound **15**, to afford compound **1** in 84% yield. ^{1}H NMR (300 MHz, CD_3CN–D_2O = 1:1, v/v) δ 8.02–8.00 (m, 1H), 7.94 (d, J = 3.0 Hz, 1H), 7.79 (d, J = 8.4 Hz, 1H), 7.65 (d, J = 8.4 Hz, 1H), 7.64 (d, J = 15.9 Hz, 1H), 7.38 (d, J = 16.5 Hz, 1H), 7.27–7.20 (m, 4H), 7.04–6.95 (m, 3H), 6.38 (t, J = 2.7 Hz, 1H), 5.42–5.33 (m, 1H), 3.64–3.46 (m, 17H), 3.09–3.02 (m, 2H), 2.44–2.35 (m, 2H), 1.63–1.38 (m, 6H), 1.27–1.81 (m, 2H), 0.83–0.73 (m, 6H). HRMS (ESI): calcd for $C_{48}H_{61}BF_2N_{10}O_8S$[M + H]$^+$, 987.4528; found, 987.4527. > 98% purity (as determined by RP-HPLC, method A, retention time = 9.54 min and 10.66 min, respectively).

*4.5. Preparation of SulfoCy7-labeled hepsin ligand (**2**)*

To a solution of SulfoCy7 NHS ester (5.0 mg, 5.90 μmol) and **15** (4.6 mg, 7.70 μmol) in DMF (2 mL) was added triethylamine (80 μL, 570 μmol). The reaction mixture was stirred at room temperature for 16 h. The reaction mixture was quenched with a mixture of ACN and water (1:1, 0.1% formic acid, 1 mL) and filtered through a 0.45 μm PTFE filter. The filtrate was purified by RP-HPLC as described for compound **15** to afford compound **2** in 50% yield. ^{1}H NMR (300 MHz, CD_3CN–D_2O = 1:1, v/v) δ 8.02 (s, 1H), 7.95 (s, 1H), 7.79–7.70 (m, 4H), 7.64 (d, J = 15.6 Hz, 1H), 7.59 (d, J = 15.6 Hz, 1H), 7.39 (s, 1H), 7.21 (d, J = 9.0 Hz, 1H), 7.18 (d, J = 9.0 Hz, 1H), 6.08 (t, J = 14.4 Hz, 1H), 5.39–5.31 (m, 1H), 3.64–3.36 (m, 20H), 3.23–3.17 (m, 2H), 3.11–3.03 (m, 2H), 2.48–2.35 (m, 6H), 2.12–2.06 (m, 2H), 1.85–1.76 (m, 2H), 1.74–1.67 (m, 2H), 1.65–1.57 (m, 16H), 1.57–1.47 (m, 2H), 1.46–1.39 (m, 2H), 1.33–1.27 (m, 2H), 1.23–1.17 (m, 2H), 0.79 (dd, J = 6.6 and 27.6 Hz, 6H). HRMS (ESI): calcd for $C_{63}H_{88}N_9O_{14}S_3$[M]$^-$, 1290.5618; found, 1290.5618. > 98% purity (as determined by RP-HPLC, method A, retention time = 3.86 and 4.20 min).

*4.6. Preparation of 4-iodobenzoic acid-labeled hepsin ligand (**18**)*

To a solution of 4-iodobenzoic acid NHS ester (7.6 mg, 22.0 μmol) and **15** (8.8 mg, 14.7 μmol) in DMF (5 mL) was added triethylamine (25 μL, 180 μmol). The reaction mixture was stirred at room temperature for 5 h. The reaction mixture was quenched with a mixture of ACN and water (1:1, 0.1% formic acid, 1 mL) and filtered through a 0.45 μm PTFE filter. The filtrate was purified by RP-HPLC as described for compound **15**, to afford compound **18** in 63% yield. ^{1}H NMR (300 MHz, CD_3CN–D_2O = 1:1, v/v) δ 8.26 (dd, J = 1.5 and 3.0 Hz, 1H), 8.19 (d, J = 3.0 Hz, 1H), 8.02 (d, J = 8.4 Hz, 1H), 8.71 (d, J = 8.4 Hz, 1H), 5.62–5.56 (m, 1H), 4.03–3.60 (m, 17H), 3.42–3.21 (m, 2H), 2.69–2.52 (m, 2H), 2.01–1.62 (m, 6H), 1.52–1.31 (m, 1H), 1.01 (dd, J = 5.4 and

13.1 Hz, 6H). HRMS (ESI): calcd for $C_{33}H_{50}IN_7O_8S[M+H]^+$, 832.2559; found, 832.2557. > 98% purity (as determined by RP-HPLC, method A, retention time = 6.72 and 7.53 min).

4.7. Determination of K_i values for hepsin inhibition

Hepsin inhibitors (15 nM–50 μM) were diluted in DMSO (2% final concentration in reaction) and mixed with activated hepsin (#4776-SE-010, R&D Systems, Minneapolis, Minnesota) to a 96-well plate (REF 353219; BD Falcon). The final assay concentration of hepsin was 0.3 nM in TNC buffer (25 mM Tris, 150 mM NaCl, 5 mM $CaCl_2$, 0.01% Triton X-100, pH 8). After incubation for 30 min at room temperature, Boc-QAR-AMC substrate (#ES014, R&D Systems, Minneapolis, Minnesota) was added to the hepsin assay solution. The final substrate concentration was 150 μM with final reaction volume of 100 μL. Changes in fluorescence (excitation at 380 nm and emission at 460 nm) were measured at room temperature over 120 min in a Biotek Synergy 2 plate reader (Molecular devices).

Hepsin activation: Based upon the manufacturer's recommendations, recombinant hepsin (#4776-SE-010, R&D Systems, Minneapolis, Minnesota) was diluted 5.5 fold in TNC buffer and incubated at 37 °C. After 24 h, the hepsin was diluted in glycerol to 50%. This stock Hepsin (1.2 μM) was stored in a −20 °C freezer and diluted in TNC buffer for use in assays. From a plot of the mean reaction velocity versus the inhibitor concentration, a non-linear curve fit was performed using GraphPad Prism version 6.04 for Windows (GraphPad Software, San Diego, CA, www.graphpad.com) to determine the inhibitor IC_{50}s from a plot of the mean reaction velocity versus the inhibitor concentration. The IC_{50} values represent the average of three separate experimental determinations. K_i values were calculated using the Cheng and Prusoff equation ($K_i = IC_{50}/(1 + [S]/K_m)$).

4.8. In vitro cell uptake study

PC3/ML and PC3/ML-Hepsin were prepared at Johns Hopkins Medical Institutions, Baltimore, Maryland. All the cell lines were maintained in DMEM supplemented with 10% FBS and 1x Pen/Strep at 37 °C in a humidified chamber with 5% CO_2. Cells were detached using 0.05% trypsin/EDTA solution and re-suspended in RPMI containing 1% FBS at 1×10^6 cells/mL cell density. Cells were incubated with the indicated concentrations of inhibitors at 37 °C for 1 h, followed by washing twice with RPMI containing 1% FBS. Cells were analyzed by BD™ LSRII Flow Cytometer (BD Biosciences, San Jose, CA) and the data were analyzed using FlowJo software (FlowJo LLC, Ashland, OR).

4.9. In silico docking studies

Ligand preparation and optimization: The 2D and 3D structure generation of all peptide ligands were each performed by *ChemBioDraw* (ver. 11.0.1) and *Chem3D pro* (ver. 11.0.1). Boron atom of BODIPY structure was replaced with sp^3 carbon during ligand preparation process because *SYBYL-X* program could not recognize boron atom for docking study. The ligands were saved as *.sdf* file. '*Surflex Searching*' preparation protocol was used to ligand preparation and optimization in *SYBYL-X* 2.1.1 (Tripos Inc., St Louis) to clean up the structures.

Protein preparation: The PDB format protein structure was downloaded from RCSB protein data bank (PDB ID: 1O5E). Protein structure preparation including conflicted side chains of amino acid residues fixation was executed by *SYBYL-X* 2.1.1. Under the application of *AMBER7 FF99* Force Field hydrogen atoms were added and minimization process was performed by *POWELL* method. Initial optimization option was set *SIMPLEX*. Default setting was applied to other parameters.

Docking and scoring function studies: To perform the docking studies of all prepared ligands, *Surflex-Dock GeomX* module was used in *SYBYL-X* 2.1.1. *Surflex-Dock* protomol as an idealized representation of a ligand guided docking to make every potential interaction with the binding site. For a generation of protomol, *Bloat (Å)* and *Threshold* were set to 0 and 0.62, respectively. All other parameters followed the default.

Declaration of Competing Interest

The authors declare no conflict of interests.

Acknowledgments

We acknowledge support from the National Research Foundation (2014R1A4A1007304 and 2017R1A2B4005036 to Y.B., and 2015R1D1A4A01016638 to S.-H.S) and from Ministry of Health & Welfare, Republic of Korea (HI16C1827 to Y.B.).

Appendix A. Supplementary material

Supplementary data to this article can be found online at https://doi.org/10.1016/j.bioorg.2019.102990.

References

[1] R.L. Siegel, K.D. Miller, A. Jemal, Cancer statistics, 2015, CA Cancer J. Clin. 65 (1) (2015) 5–29.
[2] A. Bill-Axelson, L. Holmberg, M. Ruutu, M. Haggman, S.O. Andersson, S. Bratell, A. Spangberg, C. Busch, S. Nordling, H. Garmo, J. Palmgren, H.O. Adami, B.J. Norlen, J.E. Johansson, Radical prostatectomy versus watchful waiting in early prostate cancer, N. Engl. J. Med. 352 (19) (2005) 1977–1984.
[3] A.J. Chang, K.A. Autio, M. Roach 3rd, H.I. Scher, High-risk prostate cancer-classification and therapy, Nat. Rev. Clin. Oncol. 11 (6) (2014) 308–323.
[4] C.M. Lee, H.J. Jeong, S.J. Cheong, E.M. Kim, D.W. Kim, S.T. Lim, M.H. Sohn, Prostate cancer-targeted imaging using magnetofluorescent polymeric nanoparticles functionalized with bombesin, Pharm. Res. 27 (4) (2010) 712–721.
[5] B. Candas, L. Cusan, J.L. Gomez, P. Diamond, R.E. Suburu, J. Levesque, G. Brousseau, A. Belanger, F. Labrie, Evaluation of prostatic specific antigen and digital rectal examination as screening tests for prostate cancer, Prostate 45 (1) (2000) 19–35.
[6] K.A. Kelly, S.R. Setlur, R. Ross, R. Anbazhagan, P. Waterman, M.A. Rubin, R. Weissleder, Detection of early prostate cancer using a hepsin-targeted imaging agent, Cancer Res. 68 (7) (2008) 2286–2291.
[7] K.M. Emonds, J.V. Swinnen, L. Mortelmans, F.M. Mottaghy, Molecular imaging of prostate cancer, Methods 48 (2) (2009) 193–199.
[8] J.R. Osborne, N.H. Akhtar, S. Vallabhajosula, A. Anand, K. Deh, S.T. Tagawa, Prostate-specific membrane antigen-based imaging, Urol. Oncol. 31 (2) (2013) 144–154.
[9] Q.T. Nguyen, R.Y. Tsien, Fluorescence-guided surgery with live molecular navigation–a new cutting edge, Nat. Rev. Cancer 13 (9) (2013) 653–662.
[10] E.M. Sevick-Muraca, Translation of near-infrared fluorescence imaging technologies: emerging clinical applications, Annu. Rev. Med. 63 (2012) 217–231.
[11] E.A. Owens, M. Henary, G. El Fakhri, H.S. Choi, Tissue-specific near-infrared fluorescence imaging, Acc. Chem. Res. 49 (9) (2016) 1731–1740.
[12] X. Gao, Y. Cui, R.M. Levenson, L.W. Chung, S. Nie, In vivo cancer targeting and imaging with semiconductor quantum dots, Nat. Biotechnol. 22 (8) (2004) 969–976.
[13] M. Hintersteiner, A. Enz, P. Frey, A.L. Jaton, W. Kinzy, R. Kneuer, U. Neumann, M. Rudin, M. Staufenbiel, M. Stoeckli, K.H. Wiederhold, H.U. Gremlich, In vivo detection of amyloid-beta deposits by near-infrared imaging using an oxazine-derivative probe, Nat. Biotechnol. 23 (5) (2005) 577–583.
[14] V. Humblet, R. Lapidus, L.R. Williams, T. Tsukamoto, C. Rojas, P. Majer, B. Hin, S. Ohnishi, A.M. De Grand, A. Zaheer, J.T. Renze, A. Nakayama, B.S. Slusher, J.V. Frangioni, High-affinity near-infrared fluorescent small-molecule contrast agents for in vivo imaging of prostate-specific membrane antigen, Mol. Imaging 4 (4) (2005) 448–462.
[15] X. Wu, H. Liu, J. Liu, K.N. Haley, J.A. Treadway, J.P. Larson, N. Ge, F. Peale, M.P. Bruchez, Immunofluorescent labeling of cancer marker Her2 and other cellular targets with semiconductor quantum dots, Nat. Biotechnol. 21 (1) (2003) 41–46.
[16] J. Constantinou, M.R. Feneley, PSA testing: an evolving relationship with prostate cancer screening, Prostate Cancer Prostatic Dis. 9 (1) (2006) 6–13.
[17] M. Esfahani, N. Ataei, M. Panjehpour, Biomarkers for evaluation of prostate cancer prognosis, Asian Pac. J. Cancer Prev. 16 (7) (2015) 2601–2611.
[18] F.H. Schroder, J. Hugosson, M.J. Roobol, T.L. Tammela, S. Ciatto, V. Nelen, M. Kwiatkowski, M. Lujan, H. Lilja, M. Zappa, L.J. Denis, F. Recker, A. Berenguer, L. Maattanen, C.H. Bangma, G. Aus, A. Villers, X. Rebillard, T. van der Kwast, B.G. Blijenberg, S.M. Moss, H.J. de Koning, A. Auvinen, Screening and prostate-cancer mortality in a randomized European study, N. Engl. J. Med. 360 (13) (2009) 1320–1328.
[19] I.M. Thompson, D.K. Pauler, P.J. Goodman, C.M. Tangen, M.S. Lucia, H.L. Parnes, L.M. Minasian, L.G. Ford, S.M. Lippman, E.D. Crawford, J.J. Crowley, C.A. Coltman, Jr., Prevalence of prostate cancer among men with a prostate-specific antigen level

≤4.0 ng per milliliter, N. Engl. J. Med. 350 (22) (2004) 2239–2246.
[20] T. Steuber, P. Helo, H. Lilja, Circulating biomarkers for prostate cancer, World J. Urol. 25 (2) (2007) 111–119.
[21] J. Luo, D.J. Duggan, Y. Chen, J. Sauvageot, C.M. Ewing, M.L. Bittner, J.M. Trent, W.B. Isaacs, Human prostate cancer and benign prostatic hyperplasia: molecular dissection by gene expression profiling, Cancer Res. 61 (12) (2001) 4683–4688.
[22] S. Netzel-Arnett, J.D. Hooper, R. Szabo, E.L. Madison, J.P. Quigley, T.H. Bugge, T.M. Antalis, Membrane anchored serine proteases: A rapidly expanding group of cell surface proteolytic enzymes with potential roles in cancer, Cancer Metastasis Rev. 22 (2–3) (2003) 237–258.
[23] S.M. Dhanasekaran, T.R. Barrette, D. Ghosh, R. Shah, S. Varambally, K. Kurachi, K.J. Pienta, M.A. Rubin, A.M. Chinnaiyan, Delineation of prognostic biomarkers in prostate cancer, Nature 412 (6849) (2001) 822–826.
[24] Q. Wu, G. Parry, Hepsin and prostate cancer, Front. Biosci. 12 (2007) 5052–5059.
[25] T.H. Bugge, T.M. Antalis, Q. Wu, Type II transmembrane serine proteases, J. Biol. Chem. 284 (35) (2009) 23177–23181.
[26] J.A. Magee, T. Araki, S. Patil, T. Ehrig, L. True, P.A. Humphrey, W.J. Catalona, M.A. Watson, J. Milbrandt, Expression profiling reveals hepsin overexpression in prostate cancer, Cancer Res. 61 (15) (2001) 5692–5696.
[27] T.A. Stamey, J.A. Warrington, M.C. Caldwell, Z. Chen, Z. Fan, M. Mahadevappa, J.E. McNeal, R. Nolley, Z. Zhang, Molecular genetic profiling of Gleason grade 4/5 prostate cancers compared to benign prostatic hyperplasia, J. Urol. 166 (6) (2001) 2171–2177.
[28] C. Stephan, G.M. Yousef, A. Scorilas, K. Jung, M. Jung, G. Kristiansen, S. Hauptmann, T. Kishi, T. Nakamura, S.A. Loening, E.P. Diamandis, Hepsin is highly over expressed in and a new candidate for a prognostic indicator in prostate cancer, J. Urol. 171 (1) (2004) 187–191.
[29] J.R. Somoza, J.D. Ho, C. Luong, M. Ghate, P.A. Sprengeler, K. Mortara, W.D. Shrader, D. Sperandio, H. Chan, M.E. McGrath, B.A. Katz, The structure of the extracellular region of human hepsin reveals a serine protease domain and a novel scavenger receptor cysteine-rich (SRCR) domain, Structure 11 (9) (2003) 1123–1131.
[30] P. Xing, J.G. Li, F. Jin, T.T. Zhao, Q. Liu, H.T. Dong, X.L. Wei, Clinical and biological significance of hepsin overexpression in breast cancer, J. Investig. Med. 59 (5) (2011) 803–810.
[31] T.R. Adib, S. Henderson, C. Perrett, D. Hewitt, D. Bourmpoulia, J. Ledermann, C. Boshoff, Predicting biomarkers for ovarian cancer using gene-expression microarrays, Br. J. Cancer 90 (3) (2004) 686–692.
[32] H. Tanimoto, Y. Yan, J. Clarke, S. Korourian, K. Shigemasa, T.H. Parmley, G.P. Parham, T.J. O'Brien, Hepsin, a cell surface serine protease identified in hepatoma cells, is overexpressed in ovarian cancer, Cancer Res. 57 (14) (1997) 2884–2887.
[33] H. Betsunoh, S. Mukai, Y. Akiyama, T. Fukushima, N. Minamiguchi, Y. Hasui, Y. Osada, H. Kataoka, Clinical relevance of hepsin and hepatocyte growth factor activator inhibitor type 2 expression in renal cell carcinoma, Cancer Sci. 98 (4) (2007) 491–498.
[34] Z. Han, P.K. Harris, D.E. Jones, R. Chugani, T. Kim, M. Agarwal, W. Shen, S.A. Wildman, J.W. Janetka, Inhibitors of HGFA, matriptase, and hepsin serine proteases: a nonkinase strategy to block cell signaling in cancer, ACS Med. Chem. Lett. 5 (11) (2014) 1219–1224.
[35] H. Kwon, Y. Kim, K. Park, S.A. Choi, S.H. Son, Y. Byun, Structure-based design, synthesis, and biological evaluation of Leu-Arg dipeptide analogs as novel hepsin inhibitors, Bioorg. Med. Chem. Lett. 26 (2) (2016) 310–314.
[36] V.C. Damalanka, Z. Han, P. Karmakar, A.J. O'Donoghue, F. La Greca, T. Kim, S. Pant, J. Helander, J. Klefstrom, C.S. Craik, J.W. Janetka, Discovery of selective matriptase and hepsin serine protease inhibitors: Useful chemical tools for cancer cell biology, J. Med. Chem. (2018).
[37] F.M. Franco, D.E. Jones, P.K. Harris, Z. Han, S.A. Wildman, C.M. Jarvis, J.W. Janetka, Structure-based discovery of small molecule hepsin and HGFA protease inhibitors: Evaluation of potency and selectivity derived from distinct binding pockets, Bioorg. Med. Chem. 23 (10) (2015) 2328–2343.
[38] P.K. Venukadasula, B.Y. Owusu, N. Bansal, L.J. Ross, J.V. Hobrath, D. Bao, J.W. Truss, M. Stackhouse, T.E. Messick, L. Klampfer, R.A. Galemmo Jr., Design and synthesis of nonpeptide inhibitors of hepatocyte growth factor activation, ACS Med. Chem. Lett. 7 (2) (2016) 177–181.
[39] M. Subedi, I. Minn, J. Chen, Y. Kim, K. Ok, Y.W. Jung, M.G. Pomper, Y. Byun, Design, synthesis and biological evaluation of PSMA/hepsin-targeted heterobivalent ligands, Eur. J. Med. Chem. 118 (2016) 208–218.
[40] R. Goswami, G. Wohlfahrt, O. Tormakangas, A. Moilanen, A. Lakshminarasimhan, J. Nagaraj, K.N. Arumugam, S. Mukherjee, A.R. Chacko, N.R. Krishnamurthy, M. Jaleel, R.K. Palakurthy, D.S. Samiulla, M. Ramachandra, Structure-guided discovery of 2-aryl/pyridin-2-yl-1H-indole derivatives as potent and selective hepsin inhibitors, Bioorg. Med. Chem. Lett. 25 (22) (2015) 5309–5314.
[41] H. Kwon, J. Han, K.Y. Lee, S.H. Son, Y. Byun, Recent advances of hepsin-targeted inhibitors, Curr. Med. Chem. 24 (21) (2017) 2294–2311.
[42] T. Yogo, K. Umezawa, M. Kamiya, R. Hino, Y. Urano, Development of an activatable fluorescent probe for prostate cancer imaging, Bioconjug. Chem. 28 (8) (2017) 2069–2076.
[43] A. Loudet, K. Burgess, BODIPY dyes and their derivatives: Syntheses and spectroscopic properties, Chem. Rev. 107 (11) (2007) 4891–4932.
[44] N. Boens, V. Leen, W. Dehaen, Fluorescent indicators based on BODIPY, Chem. Soc. Rev. 41 (3) (2012) 1130–1172.
[45] H. Lu, J. Mack, Y. Yang, Z. Shen, Structural modification strategies for the rational design of red/NIR region BODIPYs, Chem. Soc. Rev. 43 (13) (2014) 4778–4823.
[46] J.A. Hendricks, E.J. Keliher, D. Wan, S.A. Hilderbrand, R. Weissleder, R. Mazitschek, Synthesis of [^{18}F]BODIPY: Bifunctional reporter for hybrid optical/positron emission tomography imaging, Angew. Chem. Int. Ed. Engl. 51 (19) (2012) 4603–4606.
[47] S. Liu, T.P. Lin, D. Li, L. Leamer, H. Shan, Z. Li, F.P. Gabbai, P.S. Conti, Lewis acid-assisted isotopic ^{18}F–^{19}F exchange in BODIPY dyes: Facile generation of positron emission tomography/fluorescence dual modality agents for tumor imaging, Theranostics 3 (3) (2013) 181–189.
[48] S. Liu, D. Li, Z. Zhang, G.K. Surya Prakash, P.S. Conti, Z. Li, Efficient synthesis of fluorescent-PET probes based on [^{18}F]BODIPY dye, Chem. Commun. (Camb) 50 (55) (2014) 7371–7373.
[49] H. Kim, K. Kim, S.H. Son, J.Y. Choi, K.H. Lee, B.T. Kim, Y. Byun, Y.S. Choe, ^{18}F-Labeled BODIPY dye: A potential prosthetic group for brain hybrid PET/optical imaging agents, ACS Chem. Neurosci. (2018).
[50] H.C. Kang, R.P. Haughland, US Patent 5187288, 1993.
[51] T. Dohi, K. Morimoto, A. Maruyama, Y. Kita, Direct synthesis of bipyrroles using phenyliodine bis(trifluoroacetate) with bromotrimethylsilane, Org. Lett. 8 (10) (2006) 2007–2010.
[52] B.A. Katz, C. Luong, J.D. Ho, J.R. Somoza, E. Gjerstad, J. Tang, S.R. Williams, E. Verner, R.L. Mackman, W.B. Young, P.A. Sprengeler, H. Chan, K. Mortara, J.W. Janc, M.E. McGrath, Dissecting and designing inhibitor selectivity determinants at the S1 site using an artificial Ala190 protease (Ala190 uPA), J. Mol. Biol. 344 (2) (2004) 527–547.